Articles

Wholly Aromatic Ether-imides. Potential Materials for n-Type Semiconductors

Theo J. Dingemans,*[,†,#] Stephen J. Picken,[⊥] N. Sanjeeva Murthy,[‡] Paul Mark,[‡] Terry L. StClair,[§] and Edward T. Samulski[||]

ICASE Structures and Materials, Mail Stop 132C, NASA Langley Research Center, Hampton, Virginia 23681-2199, Physics Department, University of Vermont, Burlington, Vermont 05405, Advanced Materials and Processing Branch, NASA Langley Research Center, Hampton, Virginia 23681-2199, Department of Chemistry, University of North Carolina at Chapel Hill, Chapel Hill, North Carolina 27599-3290, and Polymers Materials and Engineering, Faculty of Applied Sciences, Delft University of Technology, Julianalaan 136, 2628 BL Delft, The Netherlands

Received November 19, 2002. Revised Manuscript Received November 19, 2003

We report on the synthesis and characterization of a series of low molar mass, high aspect ratio ether-imide compounds. All ether-imides were obtained by terminating the appropriate dianhydride, that is, pyromellitic dianhydride (**PMDA**), 1,4,5,8-naphthalenetetra-carboxylic dianhydride (**NDA**), 3,3′,4,4′-biphenyltetracarboxylic dianhydride (**BPDA**), and 3,3′,4,4′-oxydiphthalic dianhydride (**ODPA**), with three flexible aryl-ether tails of different chain lengths. Increasing the number of meta-substituted aryl-ether units reduces the melt transition temperatures and at the same time increases the solubility of the ether-imides. When the flexibility of the dianhydride moiety increases, the thermal behavior of the compounds becomes significantly more complex: The **BPDA**- and **ODPA**-based compounds form glasses and exhibit multiple crystal phases. Most compounds form isotropic melts upon heating; however, 2,7-bis(-4-phenoxy-phenyl)-benzo[*lmn*][3,8]phenanthroline-1,3,6,8-tetraone (**NDA-n$_0$**) displays a smectic A (S_A)-type texture when cooled from the isotropic phase, followed by what appears to be a smectic phase with a columnar arrangement of the mesogens inside the layers. Single-crystal X-ray diffraction analysis and cyclic voltammetry experiments indicate that the wholly aromatic ether-imides **NDA** and **BPDA** could be excellent candidates for n-type semiconductor applications.

1. Introduction

Poly(ether-imide)s (PEIs) are a well-known class of engineering plastics with outstanding mechanical properties, high thermal stability, and excellent chemical resistance toward a wide range of solvents.[1,2] PEI films are used extensively in a variety of electronic applications, that is, insulating layers, circuit boards, and low dielectric coatings.[2] In recent years, new applications for wholly aromatic ether-imides have emerged. Several groups have demonstrated that PEIs with naphthalene and perylene moieties can be used as electrochromic polymers, which some day may find use in variable reflectance mirrors[3] and organic light-emitting diodes (OLEDs).[4] More recently, Katz and co-workers demonstrated that low-molecular-weight imides can be used in organic n-type semiconductor devices such as field-effect transistors (FETs).[5] Their naphthalene-based imides with terminal fluorinated tails show high electron mobilities (>0.1 cm^2 V^{-1} s^{-1}) and excellent on/off current ratios (>10^5), even in the presence of air. Although perfluorinated copper phthalocyanines, perylene-bisimides, and α,α′-diperfluorohexyl-substituted sexithiophene-based compounds[4] appear promising as well, it seems that most devices based on n-type organic materials fail because the presence of oxygen limits the lifetime of these devices. The close molecular packing

* To whom correspondence should be addressed.
† ICASE Structures and Materials, NASA Langley Research Center.
‡ University of Vermont.
§ Advanced Materials and Processing Branch, NASA Langley Research Center.
|| University of North Carolina at Chapel Hill.
⊥ Delft University of Technology.
New address: Delft University of Technology, Faculty of Aerospace Engineering, Kluyverweg 1, 2629 HS Delft, The Netherlands. Phone: +31-15-2784520. Fax: +31-15-2784472. E-mail: t.j.dingemans@lr.tudelft.nl.

(1) Cotter, R. J. *Engineering plastics, A handbook of polyaryl ethers*; Gordon and Breach Publishers: New York, 1995.
(2) Ghosh, M. K.; Mittal, K. L. *Polyimides, fundamentals and applications*; Marcel Dekker: New York, 1996.
(3) Mackinnon, S. M.; Wang, Z. Y. *J. Polym. Sci., Part A: Polym. Chem.* **2000**, *38*, 3467.
(4) Würthner, F. *Angew. Chem., Int. Ed.* **2001**, *40*, 1037.
(5) Katz, H. E.; Lovinger, A. J.; Johnson, J.; Kloc, C.; Siegrist, T.; Li, W.; Lin, Y.-Y.; Dodabalapur, A. *Nature* **2000**, *404*, 478.

10.1021/cm021723f CCC: $27.50
Published on Web 02/20/2004

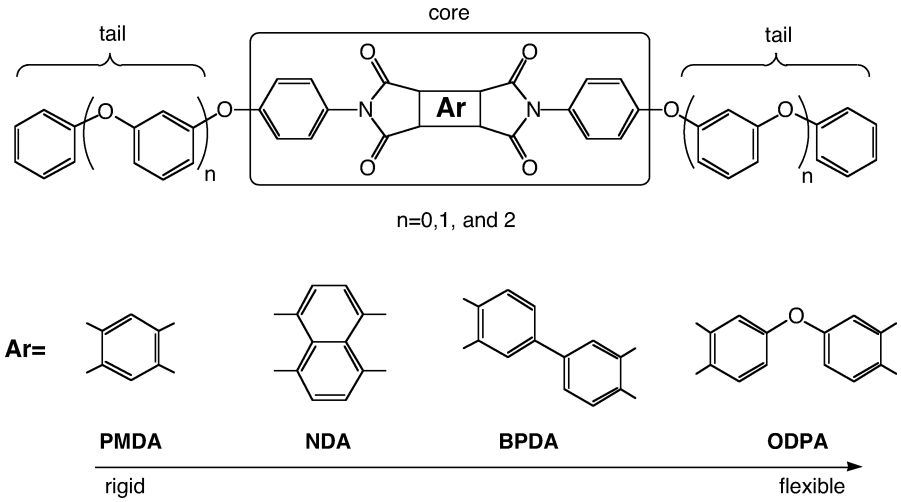

Figure 1. Ether-imide model compounds. **PMDA** = pyromellitic dianhydride, **NDA** = 1,4,5,8-naphthalenetetracarboxylic dianhydride, **BPDA** = 3,3′,4,4′-biphenyltetracarboxylic dianhydride, **ODPA** = 3,3′,4,4′-oxydiphthalic dianhydride.

in the fluorinated imides synthesized by the Katz group, however, is believed to prevent oxygen and moisture permeation and improve device lifetime and performance.

On the basis of these promising results, we believe that wholly aromatic imide-based liquid crystals would provide several advantages over nonmesogenic compounds. Liquid crystals are well-known for their outstanding barrier properties, and when designed properly, their unique packing motives could result in improved charge-carrier mobilities. Conceivably, rigid aromatic dianhydrides terminated with an appropriate aryl-ether amine could possess these useful liquid-crystalline properties. Although some groups have reported on low-molecular-weight imide-based liquid crystals,[6,7] these compounds contain aliphatic units, which lack the oxidative stability necessary for semiconductor applications. To address this problem, we recently published our results on a series of soluble low-molecular-weight imides with terminal fluorinated tails,[8] but to date, no wholly aromatic polymeric or low molecular weight ether-imide liquid crystals have been reported in the literature.

To this end, we report on the synthesis and characterization of a series of ether-imide compounds, which exhibit the classic calamitic "tail-core-tail" structure.[9] As shown in Figure 1, we have terminated four dianhydrides, that is, pyromellitic dianhydride (**PMDA**), 1,4,5,8-naphthalene-tetracarboxylic dianhydride (**NDA**), 3,3′,4,4′-biphenyltetracarboxylic dianhydride (**BPDA**), and 3,3′,4,4′-oxydiphthalic dianhydride (**ODPA**), with a homologous series of meta-substituted aryl-ether amines and studied the melt behavior, phase type, solubility, and electronic properties of these compounds.

We designed the wholly aromatic aryl-ether amines, 4-phenoxy-phenylamine ($n = 0$), 4-(3-phenoxy-phenoxy)-phenylamine ($n = 1$), and 4-(3-phenoxy-3-phenoxy-phenoxy)-phenylamine ($n = 2$), with the following rationale in mind. The terminal *p*-phenylamine functionality initially increases the aspect ratio of the resulting di-imide rigid core, while the bulky meta-substituted aryl-ether flexible units would provide the flexible tail. Also, the latter will reduce the melt transition of the high-melting di-imide rigid core and stabilize the molecular orientations necessary for mesophase formation. Aryl-ether flexible tails have not been used previously as flexible tail segments in liquid crystals, and compared to typical alkyl or alkyloxy flexible tails, aryl-ether tails have more breadth, which keeps the overall diameter of the mesogens more uniform.

2. Results and Discussion

Both flexible aryl-ether amines were prepared in acceptable overall yields. All target compounds were conveniently synthesized in one step. The ether-imides with $n = 0$ were reported before and were used as monomers toward aromatic ether-ketone polymers[10,11] or as model compounds for spectroscopic molecular modeling studies.[12−15] Compounds reported in this study, where $n = 1$ or 2, are believed to be new compounds. We found that all **PMDA**-based ether-imides (with $n = 0$, 1, and 2) showed limited solubility in common chlorinated solvents (CH_2Cl_2 and $CHCl_3$), but appear soluble in hot DMSO and 1,2-dichlorobenzene. All **NDA**-, **BPDA**-, and **ODPA**-based compounds (with $n = 0$, 1, and 2) show excellent solubilities in THF, CH_2Cl_2, and $CHCl_3$. The model compounds were recrystallized from a variety of solvents, or solvent mixtures, and the details can be found in the Supporting Information.

Thermal Properties. The phase behavior and DSC results of the pyromellitic dianhydride (**PMDA**)-, 1,4,5,8-naphthalenetetracarboxylic dianhydride (**NDA**)-, 3,3′,4,4′-biphenyltetracarboxylic dianhydride (**BPDA**)-, and 3,3′,4,4′-oxydiphthalic dianhydride (**ODPA**)-based ether-

(6) Bialecka-Florjanczyk, E.; Orzeszko, A. *J. Mater. Chem.* **2000**, *10*, 1527.
(7) Eiselt, P.; Denzinger, S.; Schmidt, H. *Liq. Cryst.* **1995**, *18*, 257.
(8) Jow, K.; Dingemans, T. *Liq. Cryst.* **2002**, *29*, 573.
(9) Collings, P. J.; Hird, M. *Introduction to liquid crystals*; Taylor and Francis: New York, 1997.
(10) Borrill, C. J.; Whiteley, R. H. *J. Mater. Chem.* **1992**, *2*, 997.
(11) Horner, P. J.; Whiteley, R. H. *J. Mater. Chem.* **1991**, *1*, 271.
(12) Wellinghoff, S. T.; Ishida, H.; Koenig, J. L.; Baer, E. *Macromolecules* **1980**, *13*, 834.
(13) Ishida, H.; Wellinghoff, S. T.; Baer, E.; Koenig, J. L. *Macromolecules* **1980**, *13*, 826.
(14) Kafafi, S. A.; Lafemina, J. P.; Nauss, J. L. *J. Am. Chem. Soc.* **1990**, *112*, 8742.
(15) Havens, J. R.; Ishida, H.; Koenig, J. L. *Macromolecules* **1981**, *14*, 1327.

Table 1. Phase Behavior, Transition Temperatures (°C), and Enthalphies (kJ mol^{-1}) (*italics*) for the Aryl-ether Terminated Di-imide Model Compounds upon Heating and Cooling (10 °C min^{-1})[a]

name	T_g	K	K′	K″	S_X	S_A	I
PMDA $n = 0$		327.6 (*8.9*)	387.4 (*60.8*)				
		361.8 (*−2.0*)	371.6 (*−60.5*)				
PMDA $n = 1$		290.3 (*87.4*)					
		286.7 (*−83.9*)					
PMDA $n = 2$		233.3 (*81.8*)					
		225.5 (*−78.2*)					
NDA $n = 0$		344.7 (*52.9*)					
		310.3 (*−23.5*)			333.3 (*−24.7*)	335.0 (*−8.0*)	
NDA $n = 1$		267.3 (*70.1*)					
		240.2 (*−45.6*)					
NDA $n = 2$		232.4 (*84.8*)					
		172.0 (*−60.5*)					
BPDA $n = 0$		203.6 (*−5.6*)	276.7 (*68.5*)				
			190.3 (*−46.3*)				
BPDA $n = 1$	69.4	118.3 (*−38.3*)	139.5 (*−6.5*)	177.6 (*62.9*)			
	63.7						
BPDA $n = 2$		145.3 (*69.3*)					
	60.8						
OPDA $n = 0$		292.4 (*73.6*)					
		244.0 (*−68.3*)					
ODPA $n = 1$	150.6	161.9 (*−7.7*)	185.2 (*46.3*)				
		141.4 (*−41.9*)					
OPPA $n = 2$	60.3	115.4 (*−35.9*)	143.3 (*37.2*)				
	56.4						

[a] T_g = glass transition temperature, K = crystal phase, S_X = unknown smectic phase, S_A = smectic A phase, and I = isotropic phase.

imides are summarized in Table 1. From these results it is evident that the meta-substituted aryl-ether flexible tails are very effective in disrupting the delicate intramolecular packing within these compounds. As the number of aryl-ether units increases, a significant reduction in melt transition is observed for all compounds. The **PMDA**- and **NDA**-based compounds are the least affected by the aryl-ether modifications. Overall, the trend is a reduction of the melt-transition temperature, but upon cooling from the isotropic, or the anisotropic, phase the molecules are able to pack into a crystal lattice almost immediately.

The **BPDA**- and **ODPA**-based compounds display moderate to severe super cooling behavior. Both **BPDA**- and **ODPA**-based ether-imides, where $n = 1$ or 2, exhibit glass-transition temperatures (T_g) and a variety of crystalline phases upon heating. Figure 2 shows the heating and cooling trace for **BPDA-n$_1$** and this scan is representative for the **BPDA** and **ODPA** series where $n = 1$ and 2.

Upon heating, a well-defined glass transition at 69 °C can be observed, followed by a crystal-to-crystal transition at 118 °C (K−K′) and this crystal phase transforms into yet another crystal form at 140 °C (K′−K″). Finally, a sharp melting endotherm indicates the solid-to-liquid transition at 178 °C (K″−I). When the isotropic melt was cooled with a cooling rate of 10 °C, an amorphous glass was formed with a T_g at 64 °C. **ODPA-n$_2$** shows a slightly lower T_g at 56 °C due to the more flexible dianhydride backbone. All transitions measured by DSC, with the exception of T_g transitions, were sharp, and this indicates that the compounds were of high purity.

Mesophase Behavior. Although the **PMDA**-, **NDA**-, and **BPDA**-based compounds have distinct features, that would promote mesophase formation, we found that

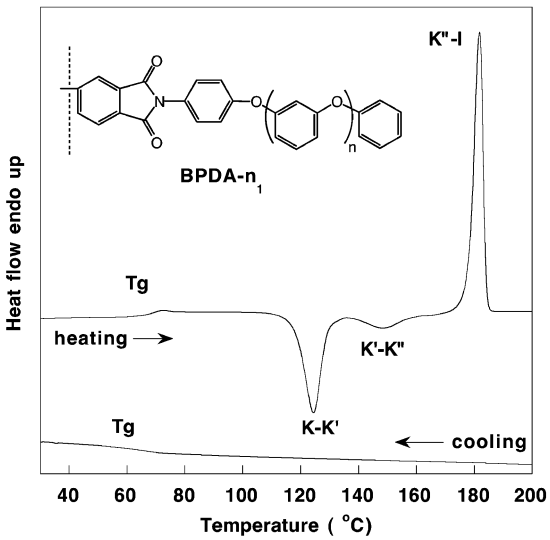

Figure 2. DSC thermogram of **BPDA-n$_1$**. Both heating and cooling scans (10 °C/min) are given. Upon heating, a T_g at 69 °C can be observed followed by two solid-state crystal transitions (K−K′ and K′−K″) and a melting endotherm (K″−I). Upon cooling, an amorphous glass is observed with a T_g of 63 °C.

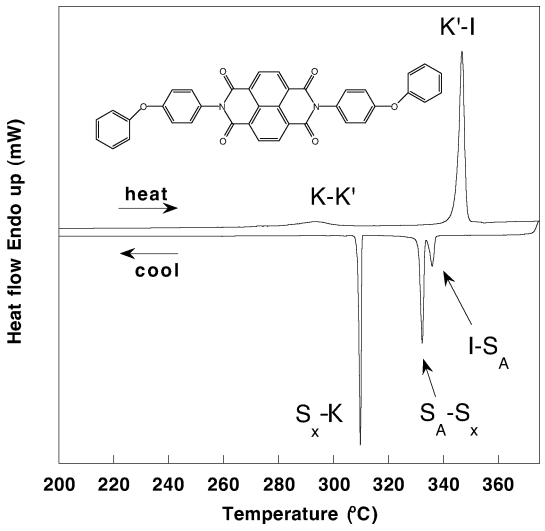

Figure 3. Second heating and cooling trace of 2,7-bis(-4-phenoxy-phenyl)-benzo[*lmn*][3,8]-phenanthroline-1,3,6,8-tetraone (**NDA-n$_0$**). The heating scan shows a crystal-to-crystal transition (K−K′) and the crystal-to-isotropic transition (K′−I); the cooling scan shows three transitions which correspond to the isotopic-to-smectic A (I−S_A), smectic A-to-smectic X (S_A−S_X), and S_X-to-crystal (S_X−K) transitions, respectively.

only one compound appeared to be mesogenic. Even more surprising is the fact that **NDA-n$_0$**, rather than **PMDA-n$_0$** or **BPDA-n$_0$**, melts into a mesophase. Eiselt et al.[7] showed that **BPDA** is an excellent mesogenic core when terminated with a variety of alkyl- or alkyloxy-phenylamines. **PMDA**, on the other hand, has been reported to form mesophases but these compounds are often too high melting (>400 °C) and are only melt-processable when long alkyloxy chains are used.[16] Although the synthesis of 2,7-bis(4-phenoxy-phenyl)-benzo[*lmn*][3,8]phenanthroline-1,3,6,8-tetraone (**NDA-n$_0$**) has been reported before,[10] the authors did not report mesophase behavior for this compound. Using 1,4,5,8-naphthalene (**NDA**) as the rigid core moiety introduces several subtle changes with respect to the overall molecular shape and electrostatics of these compounds. The shape of the rigid core widens—and hence lowers the aspect ratio—which usually destabilizes mesophase formation.[9] Instead of linking the flexible aryl-ether tails through a five-membered anhydride, a six-membered anhydride is formed. The latter is expected to have improved conjugation through the four-membered di-imide core as demonstrated by Havens et al.,[15] and this is believed to have a stabilizing effect on mesophase formation.[17] Figure 3 shows a DSC heating and cooling scan of 2,7-bis(4-phenoxy-phenyl)-benzo[*lmn*][3,8]phenanthroline-1,3,6,8-tetraone (**NDA-n$_0$**).

Optical Microscopy Results. The melt behavior of all compounds was investigated using polarizing optical microscopy. Although the model compounds can be viewed as classic "tail-core-tail" mesogens, we only observed mesomorphism in **NDA-n$_0$**. The textures of **NDA-n$_0$** are summarized in Figure 4.

The phase behavior for **NDA-n$_0$** is monotropic; that is, mesomorphism was observed upon cooling only. Figure 4a shows the formation of smectic A (S_A) batonnets at 335 °C when **NDA-n$_0$** was slowly cooled (2 °C min^{-1}) from the isotropic melt. This texture evolved rapidly into a typical smectic A (S_A) focal conic texture, shown in Figure 4b, but this phase is only stable over a 3 °C temperature range. When cooling was continued, the focal conic texture transformed into an "oak leaf"-like texture, which coexisted with dark homeotropic aligned regions, as shown in Figure 4c,d. These textures are very similar to the textures observed in columnar liquid crystals at the Col−I transition.[18,19] At 330 °C most homeotropic regions had disappeared and a stable fully developed planar aligned texture was obtained, as can be seen in Figure 4e. Figure 4f shows the same region after crystallization at 310 °C and is denoted K.

X-ray Diffraction Results. To gain more insight into the phase behavior of **NDA-n$_0$**, we performed temperature-dependent X-ray diffraction experiments on an unaligned sample. **NDA-n$_0$** was heated into the isotropic phase (∼360 °C) and slowly cooled into the LC phase. Figure 5 shows the X-ray diffraction patterns recorded during cooling.

Upon slow cooling of **NDA-n$_0$** from the isotropic phase into the S_A phase, we observed a broad diffuse halo in the wide-angle region at ∼5.1 Å, which is indicative of the liquidlike order of this phase. In the small-angle region at 335 °C, Figure 5a, a single peak appeared, which corresponds to a smectic layer spacing of 25.2 Å. On the basis of the single-crystal X-ray diffraction results, we found that the molecular length of **NDA-n$_0$** is 24.8 Å, and this indicates that the molecules pack in a typical SmA1 architecture.[20]

(16) Adduci, J. M. *Polym. Prepr.* **1990**, *31*, 63.
(17) Dingemans, T.; Murthy, N. S.; Samulski, E. T. *J. Phys. Chem. B* **2001**, *105*, 8845.
(18) Chien, C.-W.; Liu, K.-T.; Lai, C. K. *J. Mater. Chem.* **2003**, *13*, 1588.
(19) Zheng, H.; Lai, C. K.; Swager, T. M. *Chem. Mater.* **1995**, *7*, 2067.
(20) Kumar, S. *Liquid Crystals. Experimental study of physical properties and phase transitions*; Cambridge University Press: Cambridge, 2001.

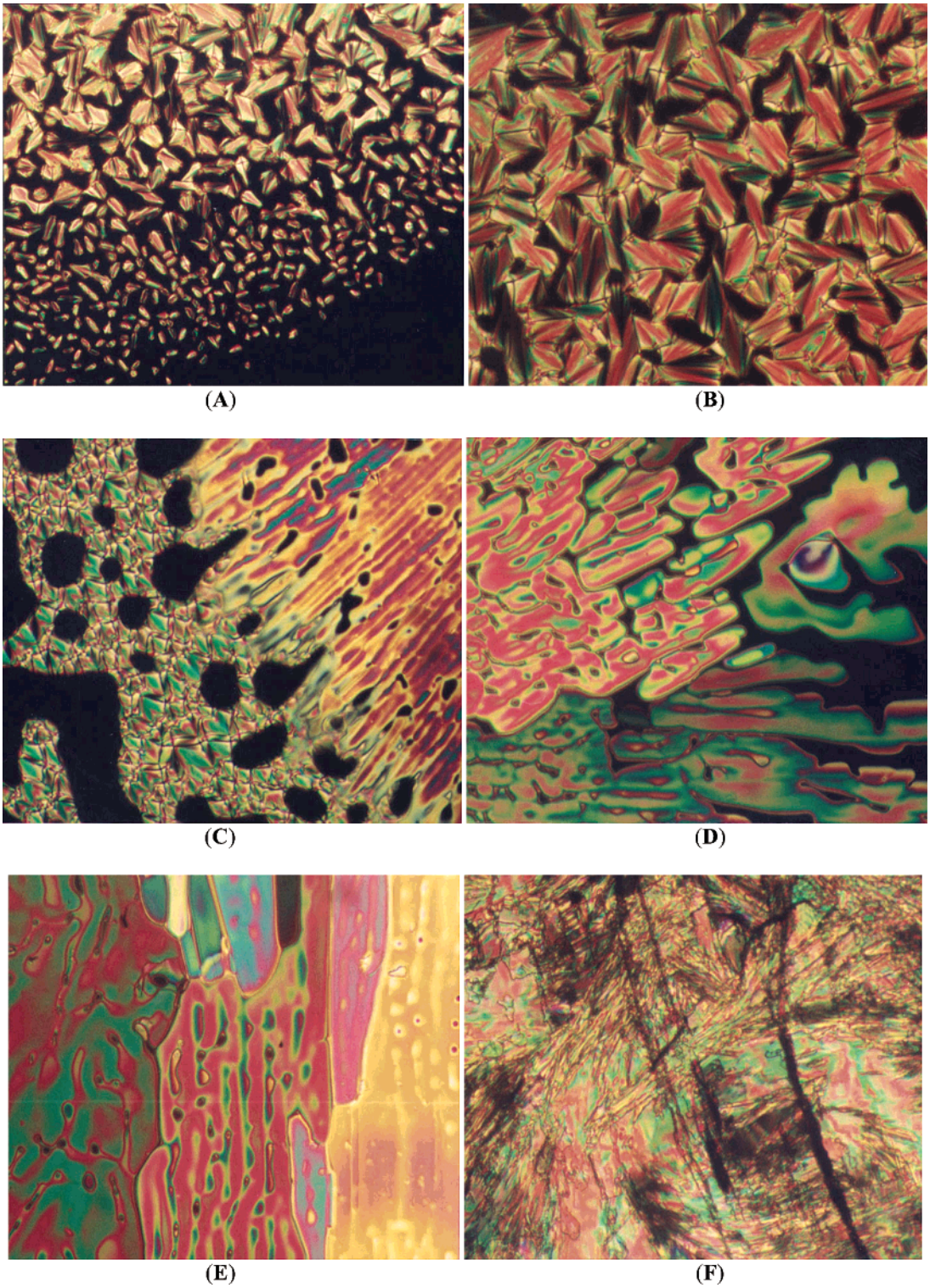

Figure 4. (A) **NDA-n$_0$** at 335 °C. Formation of batonnets upon cooling from the isotropic phase (crossed polars and 20X). (B) **NDA-n$_0$** at 334 °C. Fully developed focal conic fans (S_A) (crossed polars and 20X). (C) **NDA-n$_0$** at 333 °C. S_A phase (left) coexisting with the smectic X (S_X) (crossed polars and 20X). (D) **NDA-n$_0$** at 330 °C. S_X phase (crossed polars and 20X). (E) **NDA-n$_0$** at 320 °C. Fully developed fernlike texture of the S_X phase (crossed polars and 20X). (F) **NDA-n$_0$** at 310 °C. Crystal phase (K) (crossed polars and 20X).

At 320 °C, Figure 5b, an additional peak starts to appear at a *d*-value of about 21 Å. This indicates that there may be some tilting of the molecules. Another option would be interdigitation; however, this seems unlikely due to the presence of the bulky phenoxy end groups. Due to the absence of any other peaks in the XRD patterns, it is difficult to be more specific on the exact nature of this phase; hence, we have labeled this phase S_X. We note, however, that the overall molecular structure of our compound is very similar to that of a LC perylene di-imide studied previously by Struijk et al.[21] Therefore, one could speculate that the structure of the columnar phase could be similar; that is, we may be dealing with a smectic phase with a columnar

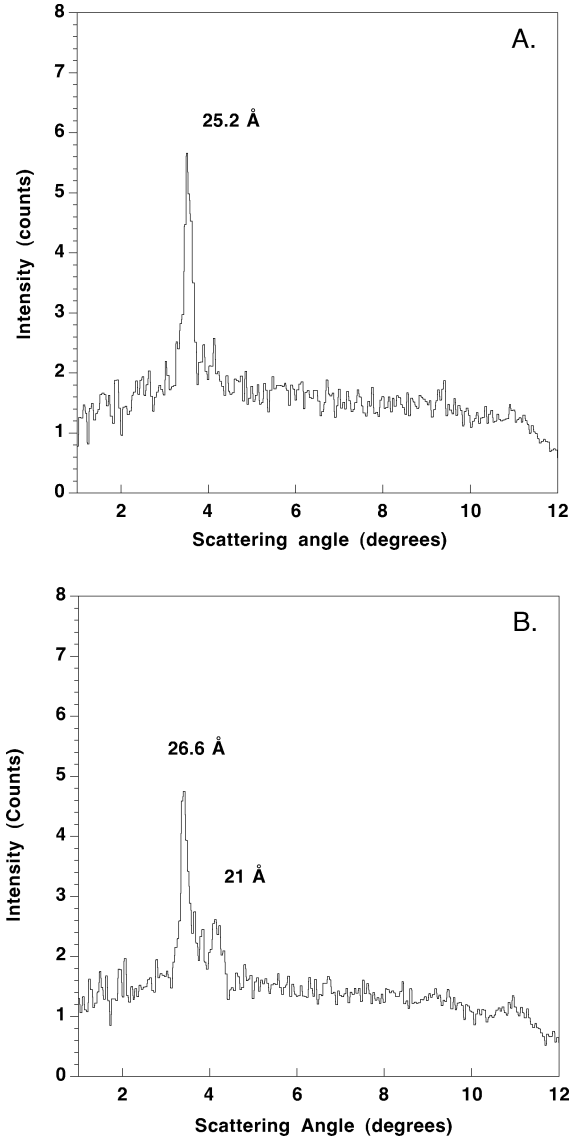

Figure 5. X-ray diffraction patterns of **NDA-n$_0$** at 335 °C (a) and 320 °C (b).

arrangement of the mesogens inside the layers. Further support for this results from the latent heat that is observed at 333 °C (i.e., 24.7 kJ/mol), which indicates a substantial change in the order of the system.

Single-Crystal X-ray Diffraction Results. We used single-crystal X-ray structure determinations to gain more detailed information about the molecular shape of our mesogenic **NDA-n$_0$** ether-imide, and to infer potential molecular packing motifs in the liquid-crystal phases. Single crystals—bright yellow platelets—of **NDA-n$_0$** were grown by slowly cooling (10 °C/h) and concentrating saturated 1,2-dichlorobenzene solutions. Figure 6 shows a perspective view of the molecular packing of **NDA-n$_0$** along the *a* and *c* axes.

The diffraction pattern in the crystalline phase could be indexed on a monoclinic unit cell of dimensions a = 7.5736 Å, b = 5.2290 Å, and c = 35.678 Å and the molecular length in this configuration was found to be

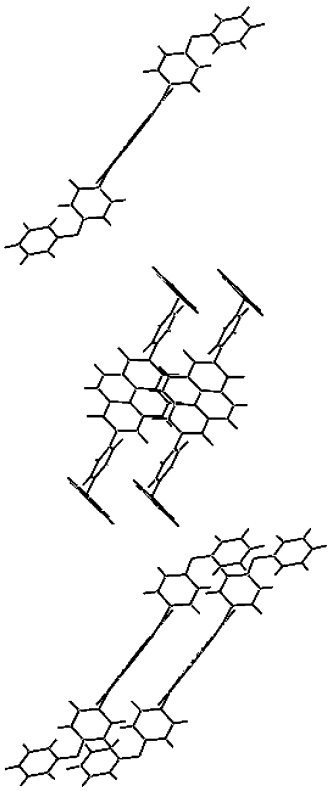

Figure 6. Crystal packing diagram of **NDA-n$_0$**. The unit cell parameters are a = 7.5736 Å, b = 5.2290 Å, and c = 35.678 Å, β = 91.251°, and Z = 2.

24.8 Å. Detailed crystal and structure refinement data are available in the Supporting Information. The distance between adjacent planar naphthalene cores is 5 Å, and this appears to be consistent with the intermolecular distance we observed in the liquid-crystal phase. Although the steric interaction between the phenyl ring and the six-membered imide ring is high, a planar conformation seems to be the preferred packing.

Katz et al. reported high electron mobilities (>0.1 cm^2 V^{-1} s^{-1}) and on/off current ratios (>10^5) for a similar **NDA**-based compound but with fluorinated tails.[5] In their case, however, the molecules preferred a herringbone packing motif while we observe a packing where the naphthalene di-imide cores adopt a coplanar packing motif. The latter, we believe, will promote π-overlap between adjacent molecules, and the combination of high stability in air and high solubility in common solvent make these ether-imide model compounds interesting candidates for n-type semiconductors.[4]

Cyclic Voltammmetry. To study the electrochemical properties and determine the LUMO levels of the ether-imides, we investigated dilute solutions of the compounds in deoxygenated tetrahydrofuran (THF) and tetrabutylammonium hexafluorophosphate (TBAPF$_6$) as a supporting electrolyte. These results are summarized in Table 2.

From the four series, only the **NDA**- and **BPDA**-based compounds showed reversible electrochemical behavior and no electrochemical polymerization after repeated scans. Both series undergo two distinct reversible reductions: the first involves the reduction of the neutral compound to the bis-anion radical and the second reduction corresponds to the formation of the tetra-anion radical species.[22] Typical voltammograms of **NDA-n$_1$**

(21) Struijk, C. W.; Sieval, A. B.; Dakhorst, J. E. J.; van Dijk, M.; Kimkes, P.; Koehorst, R. B. M.; Donker, H.; Schaafsma, T. J.; Picken, S. J.; van de Craats, A. M.; Warman, J. M.; Zuilhof, H.; Sudhölter, E. J. R. *J. Am. Chem. Soc.* **2000**, *122*, 11057.

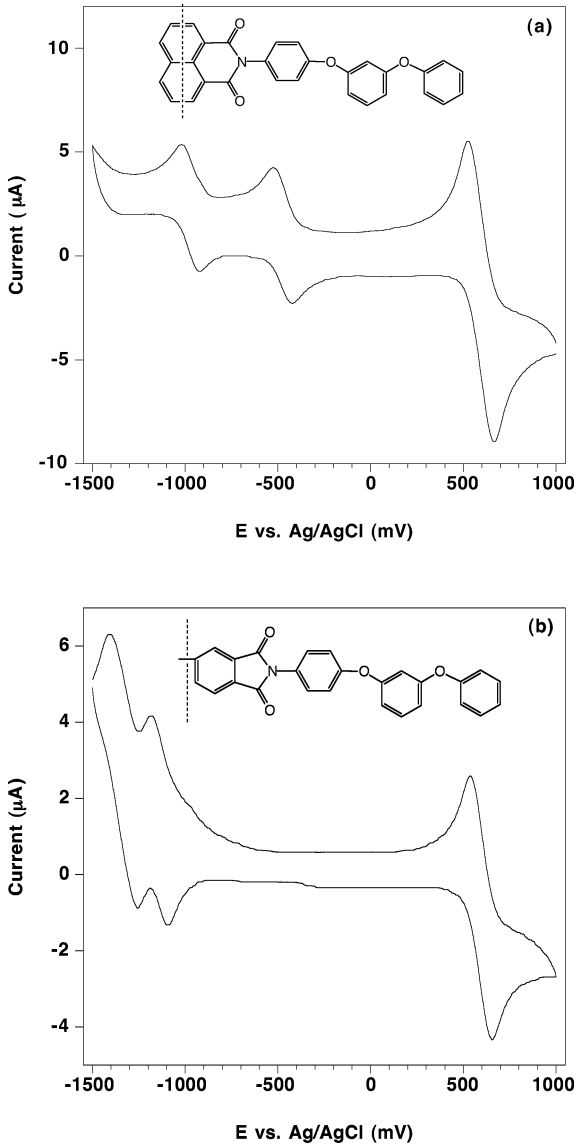

Figure 7. Typical cyclic voltammograms of **NDA-n$_1$** (a) and **BPDA-n$_1$** (b) with ferrocene in THF at room temperature. Scan rate: 100 mV s^{-1}.

Table 2. Reduction Potentials of NDA- and BPDA-Based Model Compounds vs Ag/AgCl in THF at 25 °C

compound	E_{red_1} vs Ag/AgCl [V]	E_{red_2} vs Ag/AgCl [V]	E_{red_1} vs FOC [V]	LUMO [eV]
NDA-n$_0$	−0.485	−0.996	−1.08	−3.72
NDA-n$_1$	−0.475	−0.971	−1.07	−3.73
NDA-n$_2$	−0.482	−0.990	−1.08	−3.72
BPDA-n$_0$	−1.125	−1.353	−1.72	−3.08
BPDA-n$_1$	−1.128	−1.346	−1.72	−3.08
BPDA-n$_2$	−1.125	−1.347	−1.73	−3.07

and **BPDA-n$_1$** in THF with ferrocene as internal standard are shown in Figure 7.

As expected, the length of the aryl-ether flexible tail does not affect the electrochemical properties of the ether-imides; rather, they improve the solubility and hence their processability. All three **NDA**-based compounds, with $n = 0$, 1, and 2, show similar reduction potentials ($E_{red_1} \sim -0.48$ V and $E_{red_2} \sim -0.99$ V vs Ag/AgCl) and these data are in close agreement with values reported for other **NDA**-based materials.[3,22] The **BPDA**-based compounds appear somewhat harder to reduce, as is reflected by their lower reduction potentials ($E_{red_1} \sim -1.13$ V and $E_{red_2} \sim -1.35$ V vs Ag/AgCl).

The LUMO levels were calculated with reference to the energy level of ferrocene (−4.8 eV) according to well-known semiempirical methods.[23] The LUMO levels of the **NDA**-based compounds were calculated to be −3.72 eV while the LUMO levels of the **BPDA**-based materials appear somewhat higher at −3.08 eV. These data suggest that both series have low electron injection barriers, which is a favorable property for n-channel semiconducting materials.

3. Conclusions

We have investigated four different dianhydrides as the central core moiety of wholly aromatic low-molecular-weight ether-imides. The dianhydrides were terminated with 4-phenoxyaniline, 4-(3-phenoxy-phenoxy)-phenylamine, and 4-(3-phenoxy-3-phenoxy-phenoxy)-phenylamine. When the number of meta-substituted aryl-ether units increases, the melt-transition temperatures of all model compounds drop sharply as a consequence of weakened intermolecular packing interactions. Some ether-imides are able to form amorphous glasses with well-defined glass-transition temperatures when cooled from the isotropic melt. Although the ether-imides have typical mesogenic features, we found that only the wholly aromatic ether-imide **NDA-n$_0$** melts into a smectic A (S_A) and a smectic phase with a columnar-like arrangement of the mesogens inside the layers. It appears that the molecular structural requirements for mesophase formation in wholly aromatic ether-imides are very subtle and these requirements were satisfied only for **NDA-n$_0$**. Cyclic voltammetry experiments indicate that the **NDA** and **BPDA** series have excellent electron injection properties, and in conjunction with their good thermal stability, this class of materials may be promising candidates for use in n-type semiconductor devices.

4. Experimental Section

4.1. Characterization. The structures of the intermediate and final products were confirmed using ^{1}H NMR and ^{13}C NMR spectroscopy. The spectra were recorded using a Bruker Avance 300 spectrometer (300 and 75.46 MHz). Infrared spectra were collected using a Nicolet Magna-IR Spectrometer 750, and mass spectra (MS) were obtained using a Hewlett-Packard 5972 spectrometer; M+ represents the molecular ion. UV−vis absorption spectra were recorded with a Perkin-Elmer (Lambda9) Spectrometer.

Transition temperatures were determined using a Perkin-Elmer Pyris differential scanning calorimeter (DSC), calibrated with indium (99.99%) (mp 156.5 °C, $\Delta H = 28.315$ J/g) and tin (99.99%) (mp 232.0 °C, $\Delta H = 54.824$ J/g). Heating and cooling scans were recorded at 10 °C/min. The melt behavior of the ether-imides was studied using an Olympus BH-2 optical microscope, equipped with a Mettler Toledo FP82H hot stage. Samples were examined between untreated glass microscope slides.

Temperature-dependent X-ray diffraction (XRD) measurements were carried out using a Bruker AXS 2-D detector

(22) Miller, L. L.; Zinger, B.; Schlechte, J. S. *Chem. Mater.* **1999**, *11*, 2313.

(23) Pommerehne, J.; Vestweber, H.; Guss, W.; Mahrt, R. F.; Bässler, H.; Porsch, M.; Daub, J. *Adv. Mater.*, **1995**, *7*, 551.

Scheme 1. Synthesis of 4-(3-Phenoxy-phenoxy)-phenylamine (2) and 4-(3-Phenoxy-3-phenoxy-phenoxy)-phenylamine (4)

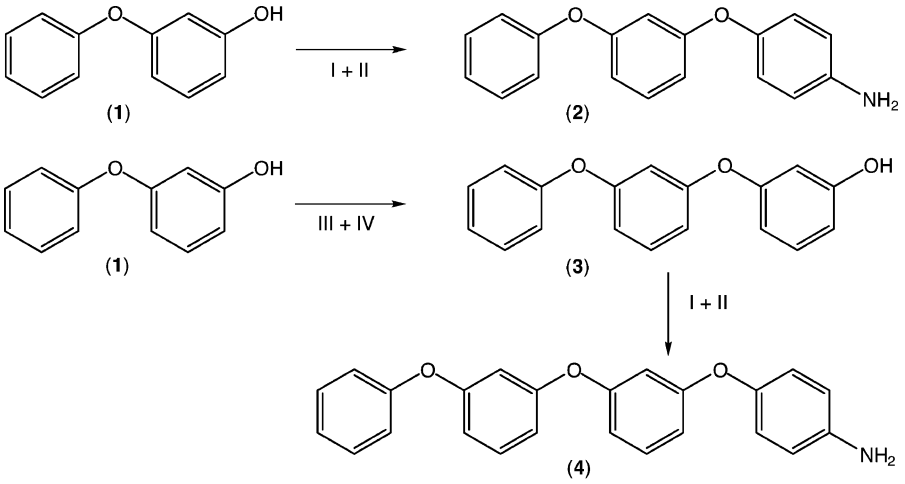

I: DMAc/K_2CO_3 and 1-fluoro-4-nitrobenzene, reflux for 12 h.
II: THF and 10% Pd-C/H_2, room temperature for 4 h.
III: Toluene/NaOMe and 3-bromoanisole/pyridine/CuCl, reflux for 12 h.
IV: HOAc and 48% HBr, reflux for 12 h.

mounted on a Rigaku sealed tube generator. The beam (Cu Kα radiation; λ = 1.542 Å) was collimated to <0.5-mm-diameter spot using a pair of Franks mirrors. Two sets of measurements were carried out, one with a sample-to-detector distance of 9.04 cm (calibration with a Si standard) and another with 23.03 cm (calibrated with Ag behenate standard). Typical exposure times of 100 s were employed for static measurements and 10 s for real-time images during cooling. The sample was placed in a 1-mm-diameter quartz capillary and sealed before data collection. The sample was heated with a hot nitrogen stream, and the sample temperature was measured using a thermocouple located near the sample.

Single-crystal data were collected on a Siemens SMART diffractometer, using the omega scan mode (Mo Kα λ = 0.71073 Å). Direct methods revealed all of the non-hydrogen atoms for **NDA-n_0** and all non-hydrogen atoms were refined anisotropically. All calculations were performed using NRCVAX software.[24]

Dilute solutions of the ether-imide model compounds in tetrahydrofuran (freshly distilled from CaH_2) were examined using cyclic voltammetry. The measurements were conducted using a Platinum (PTE) working electrode in tetrahydrofuran containing 0.1 M tetrabutylammoniumhexafluorophosphate ($TBAPF_6$). Nitrogen was bubbled through the solution to remove all traces of oxygen. The setup consisted of a three-electrode cell (BAS C-3 cell stand) and potentiostat assembly (BAS 100 B/W). The potentials were measured vs Ag/AgCl as a reference electrode and each measurement was calibrated with ferrocene as an internal standard.[23]

4.2. Materials. All common start materials and reagents were obtained from Aldrich Chemical Co. 3-Phenoxy-phenol was purchased from Alfa Aesar, pyromellitic dianhydride (**PMDA**) and 3,3′,4,4′-biphenyltetracarboxylic dianhydride (**BPDA**) from Chriskev Company Inc., and 3,3′,4,4′-oxydiphthalic dianhydride (**OPDA**) from Occidental Chemical Corporation. Toluene and pyridine were dried over and distilled from CaH_2 prior to use. From the aryl-ether amines used in this study, only 4-phenoxy-phenylamine was commercially available. 4-(3-Phenoxy-phenoxy)-phenylamine (**2**) and 4-(3-phenoxy-3-phenoxy-phenoxy)-phenylamine (**4**), however, were synthesized using standard ether synthesis procedures as shown in Scheme 1.

4-(3-Phenoxy-phenoxy)-phenylamine (**2**) was conveniently prepared in two steps by the aromatic nucleophilic displacement reaction of 3-phenoxy-phenol with 1-fluoro-4-nitrobenzene.[25] The obtained 1-(4-nitro-phenoxy)-3-phenoxy-benzene was reduced to the corresponding amine using 10% Pd/C in a hydrogen atmosphere at room temperature. The synthesis of 4-(3-phenoxy-3-phenoxy-phenoxy)-phenylamine (**4**) proved to be more elaborate. In the first step the intermediate 3-(3-phenoxy-phenoxy)-anisole was synthesized in good yields using standard Ullmann condensation techniques.[26−28] After cleaving the methoxy group with HBr,[28] the 3-(3-phenoxy-phenoxy)-phenol (**3**) was treated with 1-fluoro-4-nitrobenzene in the presence of potassium carbonate, and after reducing the nitro group, the desired amine (**4**) was obtained.

4.3. Synthesis. 4.3.1. 4-(3-Phenoxy-phenoxy)-phenylamine (2). A 300-mL two-neck flask equipped with an overhead stirrer, nitrogen inlet, and a Dean−Stark trap with condenser was charged with 9.31 g (0.05 mol) of 3-phenoxy-phenol (**1**), 7.6 g (0.055 mol) of finely ground K_2CO_3, 100 mL of DMAc, and 100 mL of toluene. This mixture was stirred and heated at 135 °C for 1.5 h, after which the temperature was increased to 175 °C. The theoretical amount of water was collected in the Dean−Stark trap and removed together with the toluene. The dark reaction mixture was cooled to room temperature, 9.2 g (0.065 mol) of 1-fluoro-4-nitrobenzene was added, and this mixture was heated to 160 °C overnight. After the reaction mixture was cooled to room temperature, 100 mL of a 15% HCl solution was slowly added. This mixture was extracted with CH_2Cl_2 (3×) and the organic layer was washed with water (2×) and dried over $MgSO_4$. After the solvent was removed, a dark yellow oil was obtained, which was purified using a Kugel-Rohr apparatus. 1-(4-Nitro-phenoxy)-3-phenoxy-benzene was obtained as a bright yellow oil at 180 °C/55 mTorr, and this material was recrystallized once from acetone (−20 °C). Yield: 10.0 g (65%). mp 54 °C. TLC (9/1 hexane/ethyl acetate) t_r = 0.5.

A 150-mL hydrogenation bottle was charged with 6.5 g (0.021 mol) of 1-(4-nitro-phenoxy)-3-phenoxy-benzene, 75 mL of dry THF, and 0.35 g of 10% Pd−C. The bottle was placed in a Parr-hydrogenator and the nitro group was reduced under a H_2-atmosphere (50 psi) at room temperature. The THF solution was filtered over a short silica gel/Celite patch and

(24) Gabe, E. J.; Le Page, Y.; Charland, J.-P.; Lee, F. L.; White, P. S. *J. Appl. Crystallogr.* **1989**, *22*, 384.

(25) Eastmond, G. C.; Paprotny, J. *Synthesis* **1998**, 894.

(26) Moroz, A. A.; Shvartsberg, M. S. *Russ. Chem. Rev.* **1974**, *43*, 679.

(27) Williams, A. L.; Kinney, R. E.; Bridger, R. F. *J. Org. Chem.* **1967**, *32*, 2501.

(28) Sax, K. J.; Saari, W. S.; Mahoney, C. L.; Gordon, J. M. *J. Org. Chem.* **1960**, *25*, 1590.

the THF was removed by distillation. A yellow oil was obtained and used without further workup. Yield: 5.7 g (97%). TLC (9/1 hexane/ethyl acetate) $t_r = 0.1$ (one spot). ^{1}H NMR ($CDCl_3$) δ (ppm): 3.85 (s, 2H), 6.65 (d, 2H, $J = 8.8$ Hz), 6.61−6.68 (m, 3H), 6.88 (d, 2H, $J = 8.8$ Hz), 7.02 (dd, 2H, $J = 8.7$ Hz), 7.09 (t, 1H, $J = 7.4$ Hz), 7.19 (t, 1H, $J = 9$ Hz), 7.32 (tt, 2H, $J = 7.5$ Hz). ^{13}C NMR ($CDCl_3$) δ (ppm): 107.84, 111.59, 112.02, 116.12, 119.0, 119.44, 121.22, 123.37, 129.67, 130.09, 142.93, 147.91, 156.72, 158.39, 160.27.

4.3.2. 4-(3-Phenoxy-3-phenoxy-phenoxy)-phenylamine (4). A 200-mL two-neck flask equipped with a stir bar, a nitrogen inlet, and a distillation apparatus was charged with 4.73 g (0.0875 mol) of sodium methoxide and 100 mL of dry toluene. With use of an addition funnel, 16.76 g (0.09 mol) of 3-phenoxy-phenol (**1**) was slowly added, and after the reaction was completed, the reaction mixture was heated and the methanol and toluene were distilled off, leaving a white phenoxy salt. The salt was cooled to room temperature, a reflux condenser was fitted on the flask, and 100 mL of dry pyridine was added. This solution was heated to reflux, and in a stream of nitrogen, 25.25 g (0.135 mol) of 3-bromoanisole was added all at once, followed immediately by 1.35 g (0.014 mol) of CuCl. This reaction mixture was stirred at reflux for 12 h and cooled to room temperature. The reaction was quenched with 80 mL of 15% HCl and extracted with diethyl ether (3×). The organic layer was washed with water and dried over $MgSO_4$. The dry ether solution was filtered over a short patch of silica gel/Celite to remove the copper salts. The solvent and excess 3-phenoxy-phenol and 3-bromoaniline were removed by vacuum distillation, and the remaining red oil was chromatographed over a short silica gel column using hexane/ethyl acetate (9/1). After the solvent was removed, 3-(3-phenoxy-phenoxy)-anisole was collected as a pale yellow oil. Yield: 15.3 g (58%). TLC (9/1 hexane/ethyl acetate) $t_r = 0.46$ (one spot). MS (m/z): 292 (M+), 249, 171, 141, 128, 115.

A 200-mL one-neck flask equipped with a stir bar and reflux condenser was charged with 15 g (0.05 mol) of 3-(3-phenoxy-phenoxy)-anisole, 150 mL of glacial acetic acid, and 80 mL of HBr (48%). This solution was refluxed for 14 h and allowed to cool to room temperature. The orange solution was extracted with CH_2Cl_2 and the organic layer was washed with water (2×) and dried over $MgSO_4$. The solvent was removed and the 3-(3-phenoxy-phenoxy)-phenol (**3**) was used for the next step without further purification. Yield: 13.5 g (94%). TLC (9/1 hexane/ethyl acetate) $t_r = 0.17$ (one spot).

A 300-mL two-neck flask equipped with an overhead stirrer, a nitrogen inlet, and a Dean−Stark trap with condenser was charged with 14.3 g (0.05 mol) of 3-(3-phenoxy-phenoxy)-phenol (**3**), 7.6 g (0.055 mol) of finely ground K_2CO_3, 100 mL of DMAc, and 100 mL of toluene. This mixture was stirred and heated at 135 °C for 1.5 h, after which the temperature was increased to 175 °C. The theoretical amount of water was collected in the Dean−Stark trap and removed together with the toluene. The dark reaction mixture was cooled to room temperature and 9.2 g (0.065 mol) of 1-fluoro-4-nitrobenzene was added. This mixture was heated to 160 °C overnight. After the reaction mixture was cooled to room temperature, 100 mL of a 15% HCl solution was slowly added. This mixture was extracted with CH_2Cl_2 (3×) and the organic layer was washed with water (2×) and dried over $MgSO_4$. After the solvent was removed, a dark yellow oil was obtained, which was dissolved in toluene. The toluene solution was chromatographed over a short silica gel column with toluene as eluent, and after the toluene was removed, a bright yellow crystalline mass was obtained. 1-(4-nitro-3-phenoxy-phenoxy)-3-phenoxy-benzene was obtained as pale yellow crystals from acetone (−20 °C). Yield: 11.2 g (70%). mp 85−87 °C. TLC (9/1 hexane/ethyl acetate) $t_r = 0.27$.

A 150-mL hydrogenation bottle was charged with 11 g (0.028 mol) of 1-(4-nitro-3-phenoxy-phenoxy)-3-phenoxy-benzene, 100 mL of dry THF, and 0.6 g of 10% Pd−C. The bottle was placed in a Parr-hydrogenator and the nitro group was reduced under a H_2 atmosphere (60 psi) at room temperature. The THF solution was filtered over a short silica gel/Celite patch and the THF was removed by distillation. A yellow oil was obtained and used without further workup. Yield: 9.85 g (95%). TLC (9/1 hexane/ethyl acetate) $t_r = 0.04$ (one spot). ^{1}H NMR ($CDCl_3$) δ (ppm): 6.65−6.76 (m, 7H), 6.78 (t, 1H, $J = 2.1$ Hz), 6.91 (d, 2H, $J = 4.4$ Hz), 7.08 (d, 2H, $J = 8.8$ Hz), 7.15 (t, 1H, $J = 7.4$ Hz), 7.24 (t, 1H, $J = 7.9$ Hz), 7.28 (t, 1H, $J = 8.1$ Hz), 7.38 (t, 2H, $J = 7.6$ Hz). ^{13}C NMR ($CDCl_3$) δ (ppm): 108.33, 109.63, 112.24, 112.57, 113.52, 113.55, 116.39, 119.37, 121.49, 123.79, 129.98, 130.40, 130.55, 143.19, 148.15, 156.83, 158.06, 158.41, 158.81, 160.54.

4.4. Synthesis of the Ether-Imide Model Compounds. All low molecular weight ether-imide compounds were synthesized in a simple one-step procedure. The appropriate dianhydride and aryl-amine were stirred in glacial acetic acid for 2 h at room temperature, followed by refluxing for 12 h. The synthesis and characterization are available in the Supporting Information.

Acknowledgment. This research was supported by the National Aeronautics and Space Administration under Contract No. NAS1-97046 while the author was in residence at ICASE, NASA Langley Research Center, Hampton, VA 23681-2199. This work was supported in part by the NASA University Research, Engineering and Technology Institute on Bio Inspired Materials (BIMat) under Award No. NCC-1-02037 and Vermont EPSCoR Grant EPS-0236976. We thank Crystal Topping for performing the DSC measurements, and Dr. Peter S. White at the University of North Carolina at Chapel Hill is gratefully acknowledged for the single-crystal X-ray diffraction studies.

Supporting Information Available: Details of the model compounds (PDF). This material is available free of charge via the Internet at http://pubs.acs.org.

CM021723F